J Nanostruct 15(3): 1354-1361, Summer 2025

RESEARCH PAPER

Prepared of CuO Nanoparticles via PLD and PLA and studied Antibacterial Activity

Saif E. Muslim*, Ahmed K. Abbas

College of Sciences, Wasit University, Wasit, Iraq

ARTICLE INFO

Article History:
Received 09 April 2025
Accepted 27 June 2025
Published 01 July 2025

Keywords:
Antibacterial Inhibition
Nanoparticles
PLA
PLA

ABSTRACT

In this study, a comparison was made between nanoparticles specifically copper oxide CuO prepared by two plasma methods, where the nanoparticles were prepared by pulsed laser ablation in a deionized liquid, and on the other hand, the nanoparticles were manufactured in the form of thin films deposited on a glass substrate where the material was evaporated in a vacuum chamber by laser. In both cases, a Nd:YAG laser was used with a wavelength of 1064 nm, and a frequency of 6 Hz. Some tests were performed on the nanoparticles such as X-ray diffraction (XRD) to study the crystal structure of the samples, as well as scanning electron microscopy (FESEM) to study the morphology of the samples and particle sizes, and optical properties (UV-VIS) to study the absorption and optical energy gaps. The samples were also tested to determine their effectiveness and use as an inhibitor of bacteria at different dilution concentrations.

How to cite this article
Muslim S., Abbas A. Prepared of CuO Nanoparticles via PLD and PLA and studied Antibacterial Activity. J Nanostruct, 2025; 15(3):1354-1361. DOI: 10.22052/JNS.2025.03.051

INTRODUCTION

Any ability to kill or inhibit bacteria or reduce bacterial growth is an antibacterial activity, and many diseases and infections are caused by these organisms. The study of this activity is very important in the development of therapeutic agents and in biomedical research, especially antibiotics, which target specific mechanisms within bacterial cells, such as cell wall synthesis, protein production, or DNA replication [1]. Antibacterial activity enters into many fields such as pharmacology, clinical microbiology, and biotechnology. [2].

In the intestines of humans and animals, there are Escherichia coli bacteria, some of which are harmful and some of which are beneficial. The restricted ones help in producing vitamins and aid in digestion. The harmful ones cause foodborne diseases with symptoms such as vomiting and diarrhea [3]. Contaminated food and water are a major source of such infections and at the same time they are useful for scientific research. [4].

One of the oxides that have antimicrobial properties is copper oxide, which makes it a promising future in medical applications due to its ability to generate reactive oxygen species. Copper oxide shows strong antibacterial activity against various pathogens [5]. Copper oxide is used in wound dressings, which helps prevent bacterial infections [6].

Advanced and widely used techniques in nanotechnology and materials science for the synthesis of nanoparticles and thin films are pulsed laser deposition and pulsed laser ablation in liquid. In PLD, the laser is directed at a target placed inside a vacuum chamber, causing the atoms to

* *Corresponding Author Email: saife@uowasit.edu.iq*

evaporate and deposit on the substrate [7]. As for PLA technology, it is a technology commonly used to create nanoparticles in liquids, known as pulsed laser ablation in liquids. This technology creates nanoparticles by scraping solid samples directly into the solution. These techniques are essential for developing advanced materials with specific properties [8].

MATERIALS AND METHODS

Nanoparticles were synthesized using pulsed laser deposition and pulsed laser ablation in liquid techniques, where the same laser parameters were used in both methods, where the wavelength was 1064 nm, the frequency was 10 Hz, and the number of shots was 300 shot.

In the PLD process, the target, which is an oxide powder, is prepared and pressed into a disc with a diameter of 1 cm and a thickness of 0.2 cm using a 5-ton hydraulic press for 5 minutes. Before the deposition process, where the glass substrates are washed with alcohol in the ultrasonic device, the target is placed in a vacuum chamber with a vacuum pressure of 10^{-2} Torr.

The laser is directed at the oxide target at a 45-degree angle, as illustrated in the accompanying Fig. 1.

In the PLAL technique, nanomaterials are synthesized in aqueous solutions, specifically distilled water. A metal specimen measuring 1 cm × 1 cm is submerged in a volume of 3 mL of the solution. The laser is directed towards the sample from a distance of approximately 10 cm, as illustrated in the Fig. 2 below. The laser parameters employed in this process are consistent with those utilized in the Pulsed Laser Deposition (PLD) method. “For bacterial testing, the nanoparticles deposited on the substrates are first scraped off, then ground, and finally dissolved in deionized water.”

Characterization of nanoparticles the nano-solution prepared using the PLA technique is deposited onto a glass substrate placed on a hot plate via drop casting. In this process, the samples prepared by both methods are deposited as thin films for subsequent testing. The crystal structure was investigated using a SHIMADZU 6000 X-ray diffractometer system. Additionally, Field Emission Scanning Electron Microscope (FE-SEM) measurements were conducted to capture atomic-scale images of the materials, making it a crucial tool in nanotechnology. The absorbance and energy band gap of the samples were determined through UV-Vis measurements. The UV-Vis measurements were conducted using a dual-beam spectrophotometer, model Shimadzu UV-1800.

Antibacterial tests After synthesizing the CuO nanoparticles, the initial concentrations for each sample were determined using Atomic Absorption Spectroscopy (AAS) and expressed in parts per million (ppm), a dilution process was carried out to achieve various concentrations. These concentrations were used to assess the impact

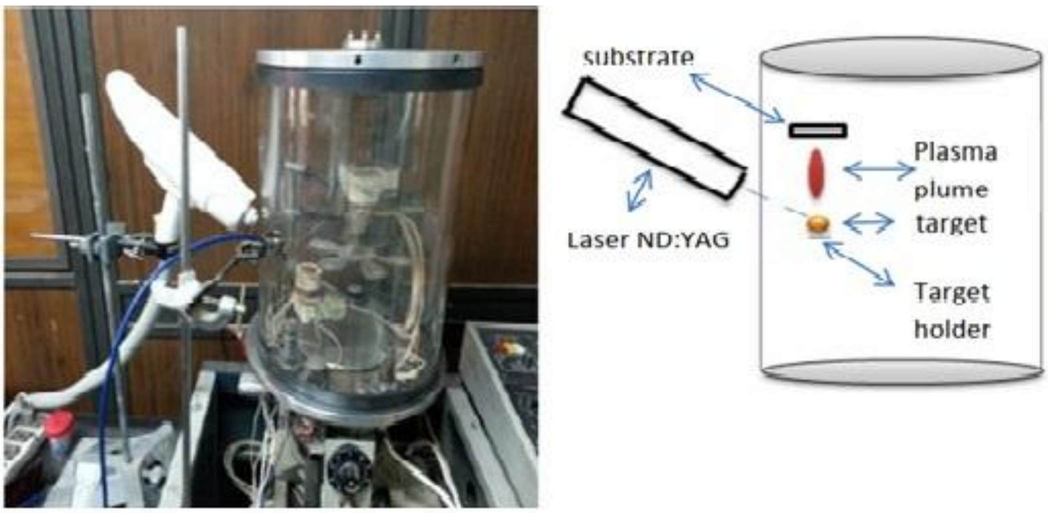

Fig. 1. PLD chamber using Nd:YAG laser.

and efficacy of each concentration on the targeted bacterial strains, with four distinct concentrations selected for each sample.

To prepare Mueller-Hinton agar, 38 grams of the powder is dissolved in 1 liter of distilled water. The mixture is then heated while continuously stirred until completely dissolved. The solution is sterilized by autoclaving at 121°C for 15 minutes. After sterilization, the solution is cooled to approximately 50°C before being poured into petri dishes. The plates are left to solidify for about 15 minutes. Once solidified, the plates are inverted and stored at 4°C.

The antibacterial activity of synthesized CuO Nano-film via pulsed laser deposition and nanoparticles by Pulsed Laser Ablation (PLA) was evaluated against Gram-negative and Gram-positive bacteria using the agar well diffusion method. Approximately 20 mL of Mueller-Hinton agar was aseptically placed in sterile Petri dishes, and bacterial strains were inoculated from stock cultures. Wells were created in the agar, and different concentrations of CuO samples were added. The plates were incubated overnight at 37°C, and the diameters of the inhibition zones were measured and recorded.

Fig. 2. PLA System using Nd:Yag laser.

Table 1. Structural parameters of CuO Nano oxide between two methods.

Sample CuO	hkl	2θ (Deg.)	FWHM (Deg.)	dhkl Exp.(Å)	C.S (nm)
PLD	(110)	32.32	3.20	2.77	2.58
	(002)	35.31	1.11	2.54	7.49
	(111)	38.70	1.07	2.32	7.90
	(112)	43.48	2.94	2.08	2.91
	(202)	48.88	0.65	1.86	13.46
	(020)	53.26	1.21	1.72	7.32
	(113)	61.45	0.98	1.51	9.41
	(311)	65.80	0.82	1.42	11.49
PLA	(002)	35.50	1.78	2.53	4.69
	(111)	38.60	1.97	2.33	4.27
	(112)	43.70	0.93	2.07	9.20

RESULTS AND DISCUSSION

The sample synthesized using the PLD technique exhibited distinct crystalline peaks at positions 32.32°, 35.31°, 38.70°, 43.48°, 48.88°, 53.40°, 58.20°, 61.50° and 67.50° on the 2θ axis. These peaks correspond to the (110), (002), (111), (112), (202), (020), (113), and (311) planes, respectively, aligning well with the reference data for CuO. Similarly, as illustrated in Fig. 3, the sample fabricated via the PLA technique displayed crystalline peaks at 35.50°, 38.60°, and 43.70°, which are associated with the (002), (111) and (112) planes, respectively. These results are consistent with [9]. This comparison highlights the structural characteristics of the CuO samples prepared by the two methods.

The data obtained reveals a noticeable contrast between the two samples prepared using different techniques as shown in table 1. The samples prepared via PLD exhibit sharper peaks with higher intensity, suggesting a more orderly and well-defined crystalline structure. In contrast, the samples prepared by PLAL show greater peak broadening, indicating possible variability in the crystal distribution or irregularities in crystal size. This analysis demonstrates the significant impact of the preparation method on the crystalline properties of the material. PLD results in higher quality crystals and less crystal size when compared to PLAL, reflecting a greater degree of crystallinity

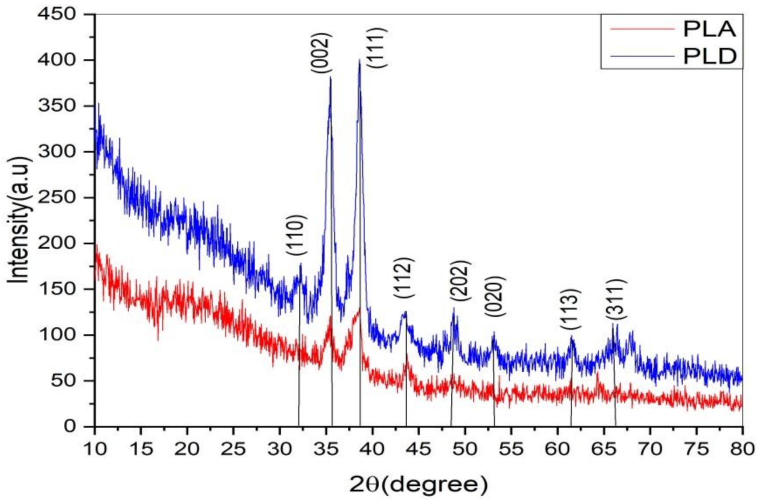

Fig. 3. XRD patterns of CuO prepared by PLAL and PLD.

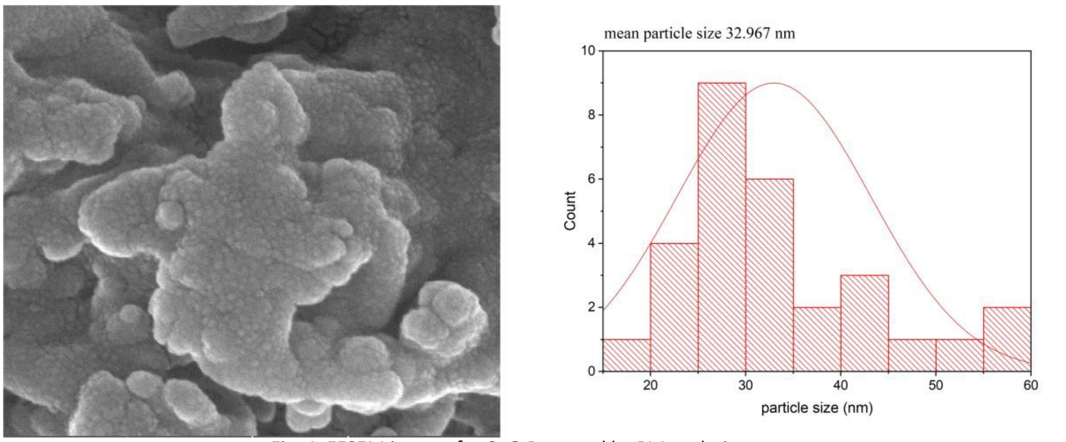

Fig. 4. FESEM images for CuO Prepared by PLA technique.

and structural uniformity in the former technique [10-11].

FESEM images confirm the distinct morphologies of the nanostructure. The images presented in the figure indicate that the synthesized CuO nanoparticles exhibit a regular spherical shape and uniform size distribution.

FESEM images confirm the diverse shapes of this nanostructure. The images presented in the figure indicate that the synthesized CuO nanoparticles exhibit a regular spherical morphology and uniform size, with an average grain size of approximately 32.967 nm have range between (20nm-60nm) for the nanoparticles prepared using the PLA method, as illustrated in Fig. 4. These findings are consistent with the results reported in reference [12].

The sample prepared using the laser deposition method was characterized through FESEM imaging, as depicted in the figure. The images reveal that the CuO NPs possess a consistent spherical morphology with uniform particle sizes. The average particle size is approximately 22.283 nm, with a size distribution ranging from 10 nm to 40 nm, as shown in Fig. 5. These results are consistent with those reported in the literature [13].

(PLAL) focuses a high-energy laser pulse onto a solid target immersed in a fluid, ablating it and creating nanoparticles distributed throughout the liquid. The liquid helps calm and stabilize the nanoparticles, often resulting in larger particles with a broader size distribution [14]. In contrast, (PLD) focuses the laser onto a solid target in a vacuum or controlled gaseous environment where the material evaporates and condenses onto the substrate [15]. This process results in more homogeneous nanoparticles due to faster condensation and the absence of a liquid medium. Therefore, nanoparticles produced by PLAL tend to be tend to be larger and more diverse in size. In contrast, nanoparticles produced by PLD are smaller and more homogeneous, benefiting from a more controlled deposition environment [16].

The absorbance of the colloidal nanoparticles was measured using UV-vis spectroscopy. The nanoparticles were synthesized using PLA at a wavelength of 1064 nm in a distilled deionized aqueous medium. The sample was then placed in a quartz cuvette using distilled deionized water as a reference. In addition, the absorbance of the same oxide of the prepared nanoparticles was determined in vacuum using the pulsed laser deposition (PLD) method, as shown in Fig. 6 below.

It is clear that the sample prepared by PLA method has higher absorption than the sample prepared by PLD method, with the absorption trending towards peak values near the green and red regions of the visible spectrum. The observed increase in absorption, as shown in the y-axis, is directly proportional to the increase in the nano-size of the materials. This increase in absorption can also be attributed to the increase in grain size and the light scattering effect resulting from the roughness of the surface of the CuO thin film [17].

The energy gap of pure copper oxide can be determined, where the energy gap values generally depend on the crystal structure of the nano oxide and the arrangement and distribution of atoms in the crystal lattice. Additionally, it is influenced by the regularity of the crystal. The energy gap value (Eg) is calculated by extrapolating the straight line from the plot of $(\alpha h\nu)^2$ vs $h\nu$ using various plasma techniques. The measurements for PLD and PLA are presented in Fig. 7.

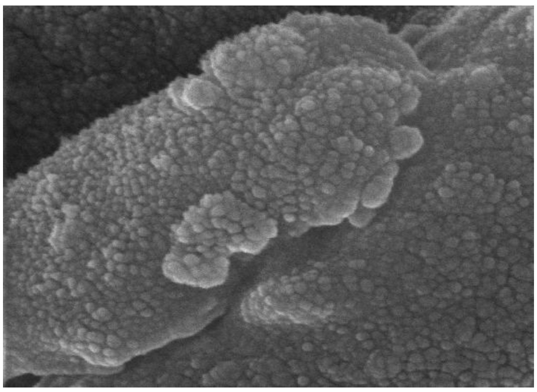

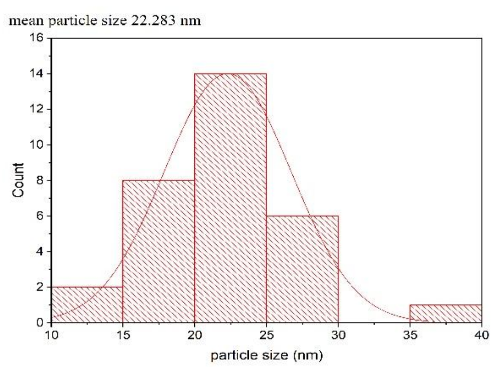

Fig. 5. FESEM images for CuO Prepared by PLD technique.

increase in band gap energy with decreasing particle size is due to the quantum confinement effect, where smaller particles restrict electron movement, causing energy levels to become quantized. This separation of energy levels raises the energy required for electrons to move to the conduction band, resulting in a larger band gap [18].

Atomic Absorption Spectroscopy (AAS), The AAS analysis was performed. Table (2) presents the concentrations of nanoparticles synthesized in distilled water using PLD and PLAL techniques for CuO.

It is evident that the particle concentration produced by the PLAL method is higher than that produced by the PLD method. This can be attributed to the fact that the PLAL technique increases the temperature of the target, which enhances the detachment of nanoparticles, facilitating their dissolution into the solution [19].

Antibacterial activity, Figs. 8 and 9 illustrate the extent of bacterial inhibition, where E. coli bacteria show a distinct inhibition zone at all four tested concentrations (12.5, 25, 50, 100 ppm) of CuO samples In both techniques. These results indicate that CuO possesses antibacterial properties, successfully limiting the growth of E. coli at different concentrations. As the concentration of CuO increases, the size of the inhibition zone also expands, demonstrating a dose-dependent antibacterial effect. This reinforces the potential of CuO as an effective antibacterial agent against E. coli.

From the above observations, it is evident that the sample prepared using the PLA method in liquid demonstrates a higher bacteriostatic effect

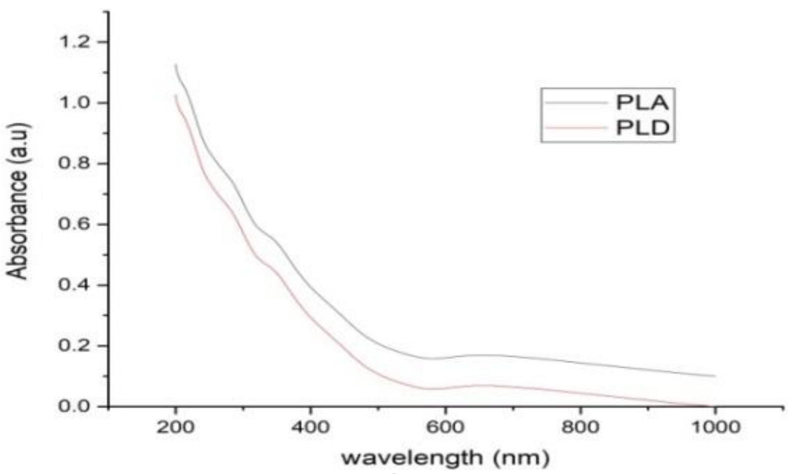

Fig. 6. UV-Visible absorbance of CuO prepared by PLA and PLD.

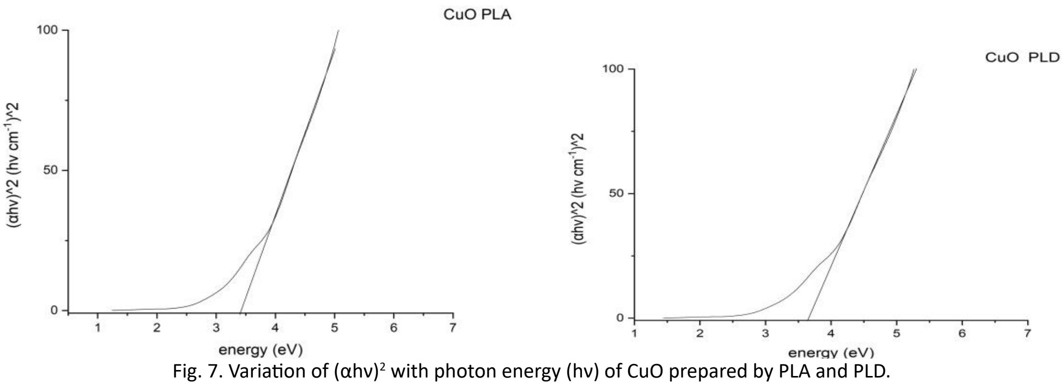

Fig. 7. Variation of $(\alpha h\nu)^2$ with photon energy (hv) of CuO prepared by PLA and PLD.

than the sample prepared by the PLD method In all concentrations In all concentrations, as shown in the table below. This disparity can be explained by the fact that the colloidal solution, which contains nanoparticles dispersed uniformly, interacts more efficiently with bacterial cells. Additionally, this can be linked to the variation in nanoparticle concentrations, as confirmed by AAS analysis. The results indicate that the inhibitory effect becomes more pronounced with increasing nanoparticle concentrations [20].

CONCLUSION

It can be concluded that the nanoparticles synthesized using the PLAL technique have a slightly larger size compared to those produced by Pulsed Laser Deposition (PLD). This size difference is mainly attributed to aggregation phenomena that occur during the interaction of the laser with matter in distilled water, leading to solutions with a higher concentration of nanoparticles compared to those synthesized via PLD. Moreover, the present study indicates that antibacterial efficacy

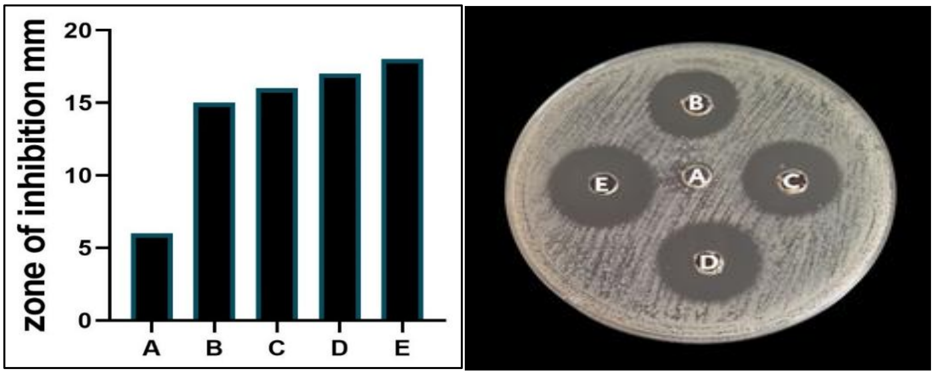

Fig. 8. Antibacterial activity of (CuO PLAL) against *E.coli.* A,

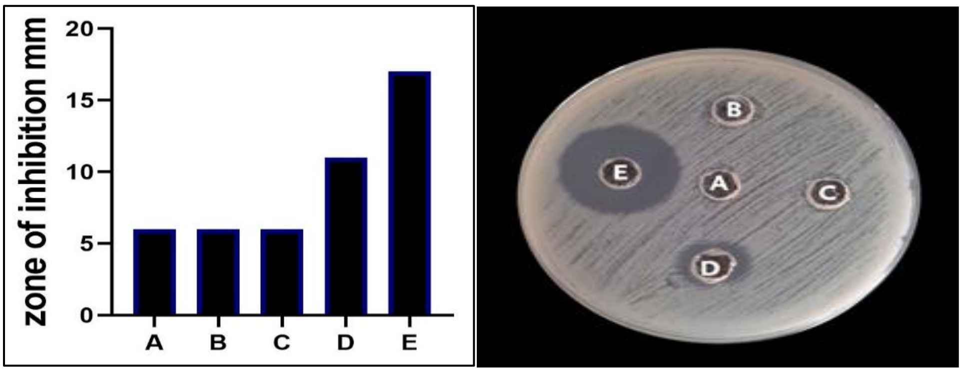

Fig. 9. Antibacterial activity of (CuO PLD) against *E.coli.* A, Control. B, 12.5 µg/mL. C, 25 µg/mL. D, 50 µg/mL. E, 100 µg/mL.

Table 2. The concentration of samples prepared by PLDand PLAL.

samples	Concentration ppm
PLAL	2.5
PLD	1.2

Table 3. Explain the antibacterial activity of nanoparticles.

	sample	A	B	C	D	E
E.coli	CuO PLAL	6	15	16	17	18.5
	CuO PLD	6	6	6	11	17

is concentration-dependent, with an increase in nanoparticle concentration correlating with enhanced bacterial inhibition.

CONFLICT OF INTEREST

The authors declare that there is no conflict of interests regarding the publication of this manuscript.

REFERENCES

1. Chandrasekaran M, Kim K, Chun S. Antibacterial Activity of Chitosan Nanoparticles: A Review. Processes. 2020;8(9):1173.
2. Farhadi F, Khameneh B, Iranshahi M, Iranshahy M. Antibacterial activity of flavonoids and their structure–activity relationship: An update review. Phytother Res. 2018;33(1):13-40.
3. Zhou Y, Zhou Z, Zheng L, Gong Z, Li Y, Jin Y, et al. Urinary Tract Infections Caused by Uropathogenic Escherichia coli: Mechanisms of Infection and Treatment Options. Int J Mol Sci. 2023;24(13):10537.
4. Gomaa EZ. Silver nanoparticles as an antimicrobial agent: A case study on Staphylococcus aureus and Escherichia coli as models for Gram-positive and Gram-negative bacteria. The Journal of General and Applied Microbiology. 2017;63(1):36-43.
5. Verma N, Kumar N. Synthesis and Biomedical Applications of Copper Oxide Nanoparticles: An Expanding Horizon. ACS Biomaterials Science and Engineering. 2019;5(3):1170-1188.
6. Sahoo J, Sarkhel S, Mukherjee N, Jaiswal A. Nanomaterial-Based Antimicrobial Coating for Biomedical Implants: New Age Solution for Biofilm-Associated Infections. ACS Omega. 2022;7(50):45962-45980.
7. Naeema N, Kudher A, Mohammed GH. Structural and Optical properties of CdTe:CuThin Films by Pulsed Laser Deposition technique. IOP Conference Series: Materials Science and Engineering. 2020;757(1):012024.
8. Altuwirqi RM. Graphene Nanostructures by Pulsed Laser Ablation in Liquids: A Review. Materials. 2022;15(17):5925.
9. Bin Mobarak M, Hossain MS, Chowdhury F, Ahmed S. Synthesis and characterization of CuO nanoparticles utilizing waste fish scale and exploitation of XRD peak profile analysis for approximating the structural parameters. Arabian Journal of Chemistry. 2022;15(10):104117.
10. Menazea AA, Mostafa AM. Ag doped CuO thin film prepared via pulsed laser deposition for 4-nitrophenol degradation. Journal of Environmental Chemical Engineering. 2020;8(5):104104.
11. Azadi H, Dizajghorbani Aghdam H, Malekfar R, Moemen Bellah S. Effects of energy and hydrogen peroxide concentration on structural and optical properties of CuO nanosheets prepared by pulsed laser ablation. Results in Physics. 2019;15:102610.
12. Dizajghorbani Aghdam H, Azadi H, Esmaeilzadeh M, Moemen Bellah S, Malekfar R. Ablation time and laser fluence impacts on the composition, morphology and optical properties of copper oxide nanoparticles. Opt Mater. 2019;91:433-438.
13. Ismail RA, Abdul Hamed RS. Decoration of copper oxide nanoplatelets with gold nanoparticles by laser ablation in methanol for photodetection applications. Optical and Quantum Electronics. 2018;50(7).
14. Shih C-Y, Shugaev MV, Wu C, Zhigilei LV. The effect of pulse duration on nanoparticle generation in pulsed laser ablation in liquids: insights from large-scale atomistic simulations. Physical Chemistry Chemical Physics. 2020;22(13):7077-7099.
15. Masood KB, Kumar P, Malik MA, Singh J. A comprehensive tutorial on the pulsed laser deposition technique and developments in the fabrication of low dimensional systems and nanostructures. Emergent Materials. 2021;4(3):737-754.
16. Theerthagiri J, Karuppasamy K, Lee SJ, Shwetharani R, Kim H-S, Pasha SKK, et al. Fundamentals and comprehensive insights on pulsed laser synthesis of advanced materials for diverse photo- and electrocatalytic applications. Light: Science and Applications. 2022;11(1).
17. Goh EG, Xu X, McCormick PG. Effect of particle size on the UV absorbance of zinc oxide nanoparticles. Scripta Mater. 2014;78-79:49-52.
18. Musa I, Qamhieh N, Mahmoud ST. Synthesis and length dependent photoluminescence property of zinc oxide nanorods. Results in Physics. 2017;7:3552-3556.
19. Fazio E, Gökce B, De Giacomo A, Meneghetti M, Compagnini G, Tommasini M, et al. Nanoparticles Engineering by Pulsed Laser Ablation in Liquids: Concepts and Applications. Nanomaterials. 2020;10(11):2317.
20. Ahmed Kadhum S. The Effect of two Types of Nano-Particles (ZnO and SiO_2) on Different Types of Bacterial Growth. Biomedical and Pharmacology Journal. 2017;10(4):1701-1708.